Mon. Not. R. Astron. Soc. **000**, 1–7 (2013) Printed 24 April 2014 (MN LATEX style file v2.2)

Evolution of dust content in galaxies probed by gamma-ray burst afterglows

Tzu-Ming Kuo,[1,2⋆] Hiroyuki Hirashita,[1] and Tayyaba Zafar[3,4]
[1]*Institute of Astronomy and Astrophysics, Academia Sinica, P.O. Box 23-141, Taipei 10617, Taiwan*
[2]*Department of Physics, National Taiwan University, Taipei 10617, Taiwan*
[3]*Aix Marseille Université, CNRS, LAM (Laboratoire d'Astrophysique de Marseille) UMR 7326, 13388, Marseille, France*
[4]*Department of Physics, University of the Punjab, Quaid-i-Azam Campus, Lahore-54590, Pakistan*

arXiv:1404.5724v1 [astro-ph.GA] 23 Apr 2014

2013 August 29

ABSTRACT
Because of their brightness, gamma-ray burst (GRB) afterglows are viable targets for investigating the dust content in their host galaxies. Simple intrinsic spectral shapes of GRB afterglows allow us to derive the dust extinction. Recently, the extinction data of GRB afterglows are compiled up to redshift $z = 6.3$, in combination with hydrogen column densities and metallicities. This data set enables us to investigate the relation between dust-to-gas ratio and metallicity out to high redshift for a wide metallicity range. By applying our evolution models of dust content in galaxies, we find that the dust-to-gas ratio derived from GRB afterglow extinction data are excessively high such that they can be explained with a fraction of gas-phase metals condensed into dust ($f_{\rm in}$) ~ 1, while theoretical calculations on dust formation in the wind of asymptotic giant branch stars and in the ejecta of Type II supernovae suggest a much more moderate condensation efficiency ($f_{\rm in} \sim 0.1$). Efficient dust growth in dense clouds has difficulty in explaining the excessive dust-to-gas ratio at metallicities $Z/{\rm Z}_\odot < \epsilon$, where ϵ is the star formation efficiency of the dense clouds. However, if ϵ is as small as 0.01, the dust-to-gas ratio at $Z \sim 10^{-2}\,{\rm Z}_\odot$ can be explained with $n_{\rm H} \gtrsim 10^6$ cm^{-3}. Therefore, a dense environment hosting dust growth is required to explain the large fraction of metals condensed into dust, but such clouds should have low star formation efficiencies to avoid rapid metal enrichment by stars.

Key words: dust, extinction — galaxies: evolution — galaxies: high-redshift — galaxies: ISM — gamma-ray burst: general

1 INTRODUCTION

One of the important problems in astrophysics is the origin and evolution of dust in the Universe, since various aspects of galaxy evolution are significantly influenced by the optical and material properties and the total abundance of dust. For example, dust governs the absorption, scattering, and reemission of the stellar light, affecting the radiative transfer in the interstellar medium (ISM) (e.g. Yajima, Umemura, & Mori 2012). Furthermore, the surface of dust grains is the main site for the formation of some molecular species, especially H_2, which could affect the star formation properties of galaxies (Hirashita & Ferrara 2002; Yamasawa et al. 2011). Therefore, clarifying the origin and evolution of dust content is essential for revealing how galaxies have evolved in the Universe.

It is widely believed that the scenario of the evolution of dust content in galaxies comprises dust formation in stellar ejecta, dust destruction in supernovae (SN) remnants, and grain growth by the accretion of metals onto preexisting grains in molecular clouds (e.g. Dwek 1998; Hirashita 1999; Inoue 2003; Zhukovska et al. 2008; Valiante et al. 2011; Mattsson & Andersen 2012). These processes depend on the age and metallicity of galaxies. In particular, the dominant mechanism of dust enrichment is suggested to switch from the supply by the stellar ejecta to the accretion of metals at a certain metallicity level (Inoue 2011; Asano et al. 2013).

For the purpose of acquiring the general trend of the evolution of dust content in galaxies at different ages and metallicities, the approaches using extinctions of bright sources of which the intrinsic spectra are well known, for example quasars (QSOs) and GRB afterglows, are regarded as viable methods, since they are bright enough to be detected even at high redshift. Quasars are usually used to probe the foreground galaxies in absorption, while GRB afterglows are often utilized to probe the ISM of their own host galaxies.

Recently, Zafar & Watson (2013) compiled and analyzed GRB afterglow data in a wide redshift range of $z = 0.1 - 6.3$. By using the $A_V/N_{\rm H}$ [A_V is the extinction at the V band (0.55 μm), and $N_{\rm H}$ is the H I column density] ratio as an indicator of dust-to-gas ratio, they show that the relation between dust-to-gas

⋆ E-mail: Raphaecaro@gmail.com

ratio and metallicity is on a natural extension of the local galaxy sample, even at low metallicities down to $Z \sim 10^{-2}$ $Z_\odot$ (Z is the metallicity and $Z_\odot$ is the solar metallicity). This indicates that the fraction of metals condensed into dust is as high as the local galaxy sample even at such a low metallicity. They did not find any systematic difference between the GRB sample and a QSO absorption sample used as a comparison sample, rejecting the systematics of the GRB sample relative to other samples. Therefore, they argue that there is a close correspondence between dust formation and metal formation; in other words, any delay between the formation of metals and dust must be shorter than typically a few Myr [i.e. the time-scale of metal enrichment by supernovae (SNe)]. They finally propose two possibilities of dominant dust formation mechanisms consistent with the close association between metals and dust: (i) rapid dust enrichment by condensation in the ejecta of SNe; and (ii) rapid grain growth by the accretion of gas-phase metals onto dust grains in the ISM.

In this study, we utilize the GRB afterglow extinction data to investigate the evolution of dust content in their host galaxies. In particular, we judge if the above two possibilities (i) and (ii) are theoretically supported or not, by applying a dust enrichment model developed in our previous studies. Through this work, we will be able to obtain or constrain some essential parameters for dust enrichment, especially, the efficiencies of dust condensation and growth.

This paper is organized as follows. In Section 2, we present the observational data adopted. In Section 3, we overview our theoretical models used to interpret the data. In Sections 4 and 5, we provide results and discussions, respectively. The conclusions are given in Section 6. In this paper, we adopt $Z_\odot = 0.02$ for the solar metallicity.

2 DATA

2.1 Extinction data of GRB afterglows

We adopt the extinction data of a sample of GRB afterglows (simply called GRBs hereafter) from Zafar & Watson (2013). They collected data from the literature for GRBs on the basis that they have: i) optical extinction estimates (derived from the X-ray-to-optical/near-infrared spectral energy distribution fitting; see Zafar et al. 2011, 2012, for the method), ii) Zn or S based metal column densities (since they are rarely condensed into dust), and iii) H I column density (wherever possible) measurements. In total, they compiled 25 GRBs with such available measurements. The models are mainly constrained by the objects whose metallicity, $N_{\rm H}$, and A_V are all detected (A_V is the rest-frame V-band extinction and $N_{\rm H}$ is the H I column density of the GRB); that is, if only an upper limit is obtained for either of those values, the data is excluded, and we are left with 9 GRBs.

Zafar & Watson (2013) compared the metals-to-dust ratios of GRBs, QSO foreground damped Lyα systems (DLAs), and galaxy-lensed QSOs to the value obtained in the Milky Way (MW), the Large Magellanic Cloud (LMC), and the Small Magellanic Cloud (SMC). They did not find any systematic difference between the GRB, QSO-DLA, and lensed galaxies samples, rejecting the systematics of the GRB sample relative to other samples. Therefore, for the uniformity of the sample, we concentrate on the GRB sample since inclusion of the QSO-DLA and galaxy-lensed QSO samples do not affect our conclusion. We refer to Vladilo (2004) for a detailed analysis of the dust evolution in DLAs.

In this paper, we focus on the relation between dust-to-gas mass ratio $\mathcal{D}$ and metallicity Z (called $\mathcal{D} - Z$ relation). To convert $A_V/N_{\rm H}$, which is used as an indicator of dust-to-gas ratio by Zafar & Watson (2013), to $\mathcal{D}$, we apply the formula explained in the next subsection. The information about extinction curve of each individual GRB is collected from the references provided in Table 1 of Zafar & Watson (2013).

2.2 Dust-to-gas ratio

In order to obtain the dust-to-gas ratio $\mathcal{D}$ from the extinction data in GRBs, we refer to the approaches established by Pei (1992). In this paper, we only consider H I for the hydrogen content, and neglect the contribution from molecular hydrogen H_2 and ionized hydrogen H II. Ionized hydrogen is unlikely to contribute largely to the total hydrogen mass (Spitzer 1978), while H_2 may have a large contribution. However, in nearby low-metallicity dwarf galaxies, molecular gas traced by CO is rarely detected, although it is not clear whether it is due to a real lack of H_2 or a different conversion factor (C may be in the form of C II rather than CO; e.g. Madden 2000). Because of such an uncertainty in H_2, we neglect the contribution from H_2. Below we briefly review the conversion formula from $A_V/N_{\rm H}$ to $\mathcal{D}$. See Pei (1992) for details.

The dust-to-hydrogen mass ratio is proportional to the extinction optical depth divided by $N_{\rm H}$ (in units of cm^{-2}) as

$$\rho_{\rm dust}/\rho_{\rm H} \equiv \chi \cdot 10^{21} (\tau_B/N_{\rm H}), \tag{1}$$

where $\rho_{\rm dust}$ and $\rho_{\rm H}$ are the mass densities of dust and hydrogen, respectively, χ is a constant depending both on the optical and material properties of dust grains, and τ_B is the extinction optical depth at the B-band (0.44 μm). Using equation (1) and converting τ_λ (extinction optical depth at wavelength λ) into A_λ (extinction at λ in units of magnitude), we obtain the following estimate for the dust-to-gas mass ratio, $\mathcal{D}$:

$$\mathcal{D} \equiv \frac{\rho_{\rm dust}}{\rho_{\rm gas}} = \frac{10^{21}}{1.4} \frac{\ln 10}{2.5} \left(\frac{1+R_V}{R_V} \right) \chi \left(\frac{A_V}{N_{\rm H}} \right) \equiv \Lambda \left(\frac{A_V}{N_{\rm H}} \right), \tag{2}$$

where $\rho_{\rm gas} = 1.4 \rho_{\rm H}$ (the factor 1.4 comes from the correction for elements other than hydrogen), $R_V \equiv A_V/(A_B - A_V)$ is the ratio of total-to-selective extinction, and Λ is referred to as the converting factor. By using the numerical values in Pei (1992), we obtain $\Lambda = 1.13 \times 10^{19}$, 1.56×10^{19}, and 2.03×10^{19} cm^{-2} mag^{-1} for the MW, LMC, and SMC extinction curves, respectively. We choose one of these three values for each object according to the extinction curve adopted by Zafar & Watson (2013) (see their Table 1).

2.3 Nearby galaxy data

Since the dust evolution models have often been 'calibrated' with nearby galaxy data (e.g. Lisenfeld & Ferrara 1998; Dwek 1998; Hirashita 1999), it would be interesting to examine if there is a difference in the $\mathcal{D} - Z$ relation between the GRB sample and nearby galaxies. For the uniformity of data, we select the samples compiled by Hirashita & Kuo (2011) (see the references therein for original data), who construct the sample based on an *AKARI* sample: eight blue compact dwarf galaxies (BCDs) and three spiral galaxies. Note that the dust content is measured by far-infrared emission, not by extinction. We also include two spiral galaxies whose dust content

is measured by extinction to confirm that there is no systematic difference in the estimate of dust content. More data are seen in e.g. Engelbracht et al. (2008): the addition of such a data set only makes the plots dense without changing the trend in the $\mathcal{D} - Z$ relation.

3 MODELS

3.1 Dust enrichment

For the purpose of investigating the evolution of dust content in a galaxy, a chemical enrichment model which describes the time evolution of gas, metals, and dust in a galaxy is adopted. We apply a simple model used by Hirashita & Kuo (2011). The simplicity of the model is the advantage for our purpose of seeing the response of the $\mathcal{D} - Z$ relation to dust formation and destruction processes. We suppose the galaxy to be a closed box; that is, we neglect inflow and outflow. The effects of inflow and outflow have only a minor effect on the $\mathcal{D} - Z$ relation (Asano et al. 2013). We also assume that the mixing of substances in galaxies is immediate and complete such that the system is treated as a one-zone environment. To make the problem analytically tractable (without losing the essence), we adopt an instantaneous recycling approximation, in which we assume that stars whose lifetimes are shorter than 5 Gyr return the gas soon after their formation. This means that we do not divide the metal and dust production by SNe and AGB stars for simplicity. Instead, we separately discuss the contributions from SNe and AGB stars in details when we interpret the results (Section 5.1). Similar kinds of analytical models are also adopted and successfully catch the essential features in the relation between dust-to-gas ratio and metallicity (Lisenfeld & Ferrara 1998; Hirashita 1999; Inoue 2003, 2011; Mattsson & Andersen 2012; Mattsson et al. 2013). For the analytic solutions and asymptotic behaviours of the models, we refer to Inoue (2011) and Mattsson et al. (2013).

The model equations are finally reduced to the relation between $\mathcal{D}$ and Z (Hirashita & Kuo 2011), since the abundances of metals and dust are tightly connected:

$$\mathcal{Y}\frac{\mathrm{d}\mathcal{D}}{\mathrm{d}Z} = f_{\mathrm{in}}(\mathcal{R}Z + \mathcal{Y}) - (\beta_{\mathrm{SN}} + \mathcal{R})\mathcal{D} + \frac{1}{\psi}\left[\frac{\mathrm{d}M_{\mathrm{dust}}}{\mathrm{d}t}\right]_{\mathrm{acc}}, \quad (3)$$

where $\mathcal{R}$ is the returned fraction of the mass from formed stars, $\mathcal{Y}$ is the mass fraction of metals that is newly produced and ejected by stars, f_{in} is the condensation efficiency of metals into dust in stellar ejecta ($f_{\mathrm{in}} = 1$ means that all the metals are condensed into dust), ψ is the star formation rate, $[\mathrm{d}M_{\mathrm{dust}}/\mathrm{d}t]_{\mathrm{acc}}$ is the rate of increase of dust mass by the accretion of metals onto preexisting grains (this term is formulated separately in Section 3.2), and β_{SN} is the efficiency of destruction of dust by shocks in SN remnants, which is defined by $\beta_{\mathrm{SN}} = \epsilon_{\mathrm{s}} M_{\mathrm{s}} \gamma/\psi$, with ϵ_{s} being the fraction of dust destroyed in a single SN blast, M_{s} being the gas mass swept per SN blast, and γ being the SN rate, as introduced by McKee (1989). Following Hirashita & Kuo (2011), we adopt $\mathcal{R} = 0.25$ and $\mathcal{Y} = 0.013$ throughout this paper, and $\beta_{\mathrm{SN}} = 9.65$ unless otherwise stated.

3.2 Grain growth by the accretion of metals onto preexisting grains

We adopt the formulation developed by Hirashita & Kuo (2011) for the increasing rate of dust mass by the accretion of metals onto preexisting grains (called grain growth hereafter):

$$\left[\frac{\mathrm{d}M_{\mathrm{dust}}}{\mathrm{d}t}\right]_{\mathrm{acc}} = \frac{\beta\mathcal{D}\psi}{\epsilon}, \quad (4)$$

where ϵ is the star formation efficiency in molecular clouds (assumed to be 0.1 unless otherwise stated), and β is the increment of dust mass in molecular clouds, which can be estimated as

$$\beta \simeq \left[\frac{\langle a^3\rangle_0}{3y\langle a^2\rangle_0 + 3y^2\langle a\rangle_0 + y^3} + \frac{1-\xi}{\xi}\right]^{-1}, \quad (5)$$

where $\xi \equiv 1 - \mathcal{D}/Z$ is the fraction of metals in gas phase, $\langle a^\ell\rangle_0$ is the ℓth moment of grain radius (we adopt $\langle a\rangle = 1.67 \times 10^{-3}$ μm, $\langle a^2\rangle = 4.68 \times 10^{-6}$ μm^2, and $\langle a^3\rangle = 7.41 \times 10^{-8}$ μm^3 based on a grain size distribution with power index -3.5 and lower and upper limits for the grain radius 0.001 and 0.25 μm, respectively; Mathis, Rumpl, & Nordsieck 1977) and $y \equiv a_0\xi\tau_{\mathrm{cl}}/\tau$, with $a_0 = 0.1$ μm being an arbitrarily given typical radius of dust grains, τ_{cl} being the lifetime of molecular clouds, and τ being the typical time-scale of grain growth. The typical time-scale of grain growth, τ, is given below in equation (6). Note that equation (4) is derived by assuming that grain growth occurs in dense molecular clouds which also host star formation. This is why the star formation efficiency enters grain growth. Since the rate of grain growth depends on the grain size distribution, β depends on the moments of grain radius as shown in equation (5). The factor $(1-\xi)$ indicates that the dust mass increases with a larger fraction if a larger part of metals are in the gas phase, and thus the term, $(1-\xi)/\xi$, expresses the saturation grain growth for $\xi \to 1$.

We adopt the following expression for τ (Hirashita & Kuo 2011, Eq. 23, applicable for silicate):

$$\tau = 6.3 \times 10^7 \left(\frac{Z}{\mathrm{Z}_\odot}\right)^{-1} a_{0.1} n_3^{-1} T_{50}^{-1/2} S_{0.3}^{-1}\ \mathrm{yr}, \quad (6)$$

where $a_{0.1} \equiv a_0/(0.1\ \mu\mathrm{m})$, $n_3 \equiv n_{\mathrm{H}}/(10^3\ \mathrm{cm}^{-3})$ (n_{H} is the number density of hydrogen nuclei), $T_{50} \equiv T_{\mathrm{gas}}/(50\ \mathrm{K})$ (T_{gas} is the gas temperature), and $S_{0.3} \equiv S/0.3$ (S is the sticking probability of the dust-composing material onto the preexisting grains. We use the same values as in Hirashita & Kuo (2011); i.e. $a_0 = 0.1$ μm, $n_{\mathrm{H}} = 10^3$ cm^{-3}, $T_{\mathrm{gas}} = 50$ K, and $S = 0.3$ unless otherwise stated. A similar time-scale is obtained for carbonaceous dust mainly because silicate and carbonaceous dust have similar total abundances of dust-composing materials (Hirashita & Kuo 2011, Eq. 24) Thus, we simply use equation (6) for τ in this paper.

By using equation (4), equation (3) can be restated as

$$\mathcal{Y}\frac{\mathrm{d}\mathcal{D}}{\mathrm{d}Z} = f_{\mathrm{in}}(\mathcal{R}Z + \mathcal{Y}) - \left(\beta_{\mathrm{SN}} + \mathcal{R} - \frac{\beta}{\epsilon}\right)\mathcal{D}. \quad (7)$$

We solve this equation to obtain the $\mathcal{D} - Z$ relation.

4 RESULTS

4.1 Overall behaviour of the $\mathcal{D} - Z$ relation

The $\mathcal{D} - Z$ relations calculated by our models above are shown for various values of f_{in} and β_{SN} in Fig. 1. The overall behaviour of the $\mathcal{D} - Z$ relation predicted by the model has already been described in Hirashita & Kuo (2011). We briefly summarize it here. In low metallicity environments, the dust is simply supplied from the dust condensation in stellar ejecta, which results in an approximately linear relation, $\mathcal{D} \sim f_{\mathrm{in}}Z$. Afterwards, when the dust-to-gas ratio $\mathcal{D}$ reaches a value about $f_{\mathrm{in}}\mathcal{Y}/\beta_{\mathrm{SN}}$, dust destruction in SNe remnants suppresses the increase of the dust, and the $\mathcal{D} - Z$ relation becomes flatter at this stage. Ultimately, in high metallicity environments, the dust-to-gas ratio $\mathcal{D}$ increases sharply because

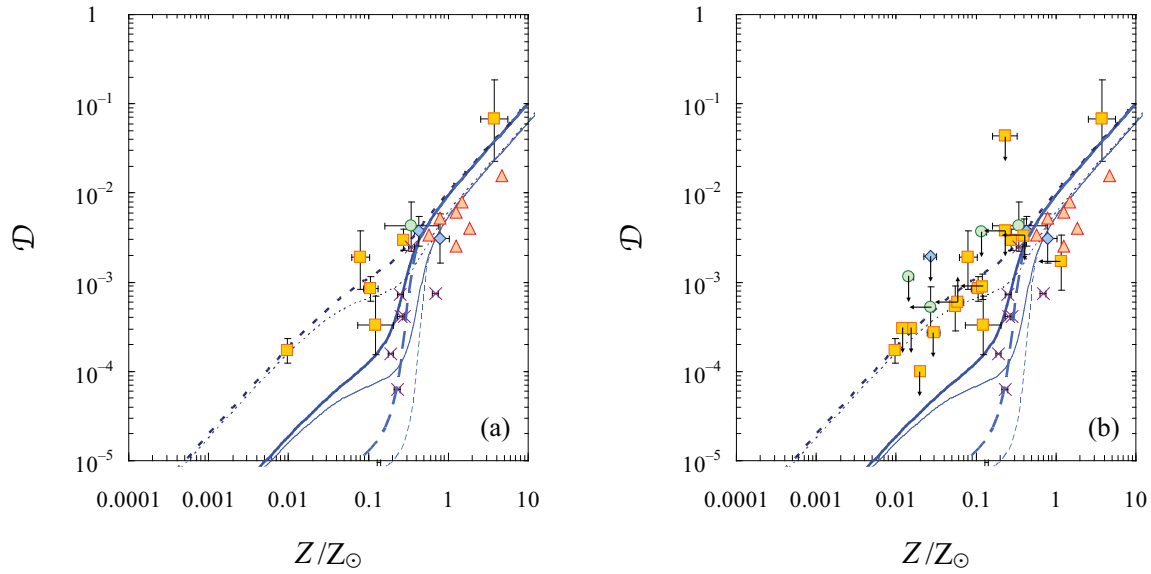

Figure 1. Relation between the dust-to-gas ratio $\mathcal{D}$ and metallicity Z. The squares, diamonds, and circles represent the GRB sample data whose dust-to-gas ratios are derived by using SMC, LMC, and MW extinction curves, respectively (Zafar & Watson 2013). The dashed, solid, and dotted lines indicate the evolution of dust content with $f_{\rm in}$ (the dust condensation efficiency of the metals in the stellar ejecta) equal to 0.01, 0.1, and 1, respectively. The thick lines are for $\beta_{\rm SN}$ (the dust destruction factor by SN) equal to 9.65, while the thin ones are with $\beta_{\rm SN} = 19.3$. For comparison, the nearby galaxy data are also shown, the crosses and triangles representing the blue compact dwarf galaxies and the spiral galaxies, respectively. Panel (a) presents data points with all detected A_V, $N_{\rm H}$, and metallicity, while Panel (b) presents all the data points, with arrows indicating upper or lower limits.

of the nonlinear increase in dust content through grain growth, i.e. $\mathrm{d}\mathcal{D}/\mathrm{d}Z \propto \mathcal{D}Z$.

4.2 Comparison with GRB afterglows

For GRBs, we first adopt merely 9 data points with both detected $[A_V/N_{\rm H}]$ and metallicity. As shown in Fig. 1, it is obvious that some data points at low metallicities can just be explained with $f_{\rm in} \sim 1$, which indicates an extremely efficient condensation of metals into dust in stellar ejecta. The possibility of such a high $f_{\rm in}$ is further discussed in terms of theoretical calculations of dust production in stellar ejecta in the literature (Section 5.1).

We also show the dependence on $\beta_{\rm SN}$ by fixing $f_{\rm in} = 1$. In Fig. 1a, we show the cases with $\beta_{\rm SN} = 9.65$ (standard value) and 19.3 (two-times efficient dust destruction). We observe that the difference appears around 0.01–0.1 $Z_\odot$; since the dust destruction rate is proportional to the dust-to-gas ratio, it is negligible compared with the dust formation in stellar ejecta at low metallicities ($\lesssim 0.01$ $Z_\odot$) (Yamasawa et al. 2011). At $Z > 0.1$ $Z_\odot$, grain growth becomes efficient. Therefore, the scatter of $\mathcal{D}$ around 0.01–0.1 $Z_\odot$ can be interpreted as different destruction efficiencies. However, we should note that this interpretation is only possible for $f_{\rm in} \sim 1$: if $f_{\rm in} \ll 1$, the inclusion of efficient SN shock destruction makes it difficult to explain the objects with relatively large $\mathcal{D}$ around $Z \sim 0.1$ $Z_\odot$.

Grain growth can raise $\mathcal{D}$. The effect of grain growth appears in Fig. 1a as a rapid increase of $\mathcal{D}$ around $Z \sim 0.1$–1 $Z_\odot$. Grain growth is prominent only for $f_{\rm in} \ll 1$, since most of the metals are already in dust grains for $f_{\rm in} \sim 1$. However, grain growth has difficulty in explaining the high dust-to-gas ratios in low-metallicity objects since grain growth becomes effective only when the ISM is significantly enriched with metals (e.g. Asano et al. 2013).

In Fig. 1b, we also show the same results including data with upper and lower limits. Two data around $Z \sim 0.02$–0.03 $Z_\odot$ with upper limits for $\mathcal{D}$ can be explained by moderate condensation efficiencies with $f_{\rm in} < 1$, so there could be some variation in $f_{\rm in}$. Other than those data points, the upper/lower limit data do not constrain the model parameters more severely than the 9 data points with detections. Thus, we hereafter focus on the 9 data points with detection in our analysis.

As shown in Fig. 1, the lines with $f_{\rm in} \sim 0.1$ is consistent with the $\mathcal{D} - Z$ relation of the nearby sample. The steep rise of $\mathcal{D}$ around $Z \sim 0.1$ $Z_\odot$ is due to grain growth. It is noteworthy that grain growth is required to explain the steep trend of dust-to-gas ratio relative to metallicity in BCDs and the relatively high dust-to-gas ratio of spiral galaxies. We also observe in Fig. 1 that, at any metallicity, the dust-to-gas ratios for GRBs are overall higher than those of BCDs or spiral galaxies. Therefore, it appears that there is a tension between the $f_{\rm in}$ value of GRBs and that of nearby galaxies.

Summarizing the results, the GRB data can be explained with $f_{\rm in} \sim 1$, which is significantly larger than the value fitting the nearby galaxies ($f_{\rm in} \sim 0.1$). In the next section, we discuss (i) the value of $f_{\rm in}$ suggested by dust condensation models in stellar ejecta; (ii) alternative explanations; and (iii) possible observational reasons for the tension between the GRB sample and the nearby galaxy sample.

5 DISCUSSION

5.1 Condensation efficiency dust in stellar ejecta

To discuss the reasonable range for the value of $f_{\rm in}$, we refer to the data compiled by Inoue (2011) for theoretical calculations on dust formation in the wind of AGB stars by Zhukovska, Gail, & Trieloff

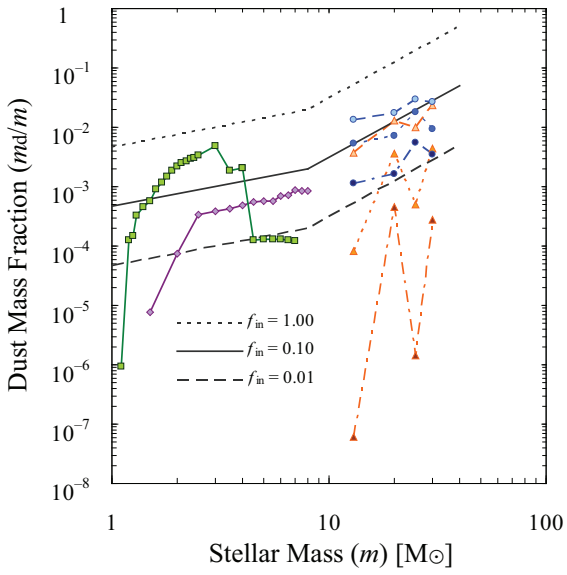

Figure 2. Ejected dust mass fraction $m_{\rm d}/m$ as a function of the stellar mass at the zero-age main sequence. For AGB dust, the data of the square points are taken from Zhukovska et al. (2008) with metallicity $Z = 0.008$, and the data of the diamond points are taken from Ventura et al. (2012) with metallicity $Z = 0.008$. For SN dust, the data of the round points are from top to bottom in sequence with hydrogen density $n_{\rm H} = 0.1$, 1, and 10 cm^{-3} for mixed helium cores, and the data of the triangular points are from top to bottom in sequence with hydrogen density $n_{\rm H} = 0.1$, 1, and 10 cm^{-3} for unmixed helium cores, both taken from Nozawa et al. (2007). The three parallel black skew lines indicate the double power-law approximations for the ejected dust mass fraction rate provided by Inoue (2011), with condensation efficiencies of metals into dust in stellar ejecta $f_{\rm in} = 1$, 0.1, and 0.01, from the upper to the lower lines, respectively.

(2008), and on dust formation in SN ejecta by Nozawa et al. (2007). We add additional data for the dust formation in AGB stars calculated by Ventura et al. (2012). Bianchi & Schneider (2007)'s models for the dust formation in SN ejecta are located in the range consistent with Nozawa et al. (2007)'s results. For Nozawa et al. (2007)'s models, we adopt ambient hydrogen number densities of 0.1, 1, and 10 cm^{-3} since more dust is destroyed (so less dust is ejected) in high-density environments. The relation between the progenitor stellar mass m at the zero-age main sequence and the dust mass produced $m_{\rm d}$ is shown in Fig. 2 ($m_{\rm d}$ is normalized to m). In order to constrain $f_{\rm in}$ from the plot, we need to assume the total metal mass ejected from a star, m_Z. We follow Inoue (2011) for the relation between m_Z/m and m:

$$\frac{m_Z}{m} = \begin{cases} 0 & (m > 40\ {\rm M}_\odot), \\ 0.02\,(m/8\ {\rm M}_\odot)^2 & (8\ {\rm M}_\odot \leqslant m \leqslant 40\ {\rm M}_\odot), \\ 0.02\,(m/8\ {\rm M}_\odot)^{0.7} & (m < 8\ {\rm M}_\odot). \end{cases} \quad (8)$$

Fig. 2 shows the lines for $m_{\rm d} = f_{\rm in} m_Z$ for various $f_{\rm in}$. We find that $f_{\rm in} \sim 0.1$ is supported on average while $f_{\rm in} = 1$ is far above all the predictions. Thus, such an extremely high condensation efficiency as $f_{\rm in} \sim 1$ as suggested by the data points of GRBs (Section 4.2) is somewhat excessive. It is interesting that $f_{\rm in} = 0.1$ is consistent with the nearby galaxy data in Fig. 1.

5.2 Grain growth

It is worth searching for an alternative solution that can explain the high dust-to-gas ratios of the GRB sample. Here, we try to explain the data with extremely efficient grain growth by adopting a moderate $f_{\rm in} \sim 0.1$. An efficient grain growth is equivalent to a short τ, which can be reasonably realized by a high $n_{\rm H}$ (equation 6). In Fig. 3a, we show the $\mathcal{D} - Z$ relation for $n_{\rm H} = 10^3$, 10^4, 10^5, and 10^6 cm^{-3}. The enhanced grain growth actually explain the data points around $Z = 0.1$ Z$_\odot$; however, the excessively large dust content of some data points at low metallicities ($Z < 0.1$ Z$_\odot$) is still not reproduced. This is because the grain growth time-scale is typically longer than the metal enrichment time-scale at such low metallicities as estimated below.

Let us compare the metal enrichment time-scale and the grain growth time-scale. After a significant gas consumption, the metallicity becomes roughly solar (e.g. Tinsley 1980). Therefore, the metal enrichment time-scale to a metallicity level of Z is estimated as $\tau_Z \sim (M_{\rm gas}/\psi)(Z/{\rm Z}_\odot)$, where $M_{\rm gas}$ is the gas mass. The grain growth time-scale is, on the other hand, $\tau_{\rm grow} \sim M_{\rm dust}/[{\rm d}M_{\rm dust}/{\rm d}t]_{\rm acc} = \epsilon M_{\rm gas}/(\beta\psi) = \epsilon\tau_{\rm Z}({\rm Z}_\odot/Z)/\beta$. At the metallicity level where grain growth becomes the dominant dust-producing mechanism, $\beta \sim 1$ (Hirashita & Kuo 2011). Thus, $\tau_Z < \tau_{\rm grow}$ for $Z/{\rm Z}_\odot < \epsilon$, which indicates that the metal enrichment occurs faster than the grain growth at $Z < 0.1$ Z$_\odot$ if $\epsilon = 0.1$ as adopted above. In other words, grain growth cannot affect the dust-to-gas ratio by the time when the system is enriched with metals up to 0.1 Z$_\odot$, as long as we adopt $\epsilon = 0.1$ derived from nearby molecular clouds (e.g. Lada, Lombardi, & Alves 2010).

The above arguments suggest that grain growth becomes efficient at even lower metallicities if we adopt smaller ϵ. In Fig. 3b, we show the results for $\epsilon = 0.01$. We observe that, considering denser gas and less efficient star formation, we can reproduce the data points at $Z < 0.1$ Z$_\odot$. This is because low star formation efficiency allows grains to grow within the metal enrichment time-scale, which is inversely proportional to the star formation efficiency. Thus, it appears that the only way to explain the dust-to-gas ratio in the GRB sample at $Z < 0.1$ Z$_\odot$ is to impose a low star formation efficiency (or equivalently to slow the metal enrichment). This implies the difference between nearby galaxies and the host galaxies of GRBs in terms of the star formation efficiency in dense clouds, although the physical mechanism of producing such a difference is not clear. Alternatively, the GRB sample is biased to objects with low star formation efficiencies, as discussed in the next subsection.

In summary, slow metal enrichment because of low star formation efficiency enable grain growth to occur within the metal enrichment time-scale even at low metallicities, so that most of the metals can be condensed into dust by grain growth. Therefore, the combination of a low star formation efficiency and an enhanced grain growth by a high density can explain the data points at low metallicities.

5.3 Comparison with the nearby galaxy sample

As shown in Fig. 1, the dust-to-gas ratios in GRBs are systematically larger than those of nearby galaxies. According to the argument in the previous subsection, a possible interpretation is that GRB host galaxies have smaller star formation efficiencies than nearby galaxies. Probably, the nearby galaxy sample is biased to star-forming objects, which are by definition forming stars actively. On the other hand, we tend to choose gas-rich galaxies by a GRB,

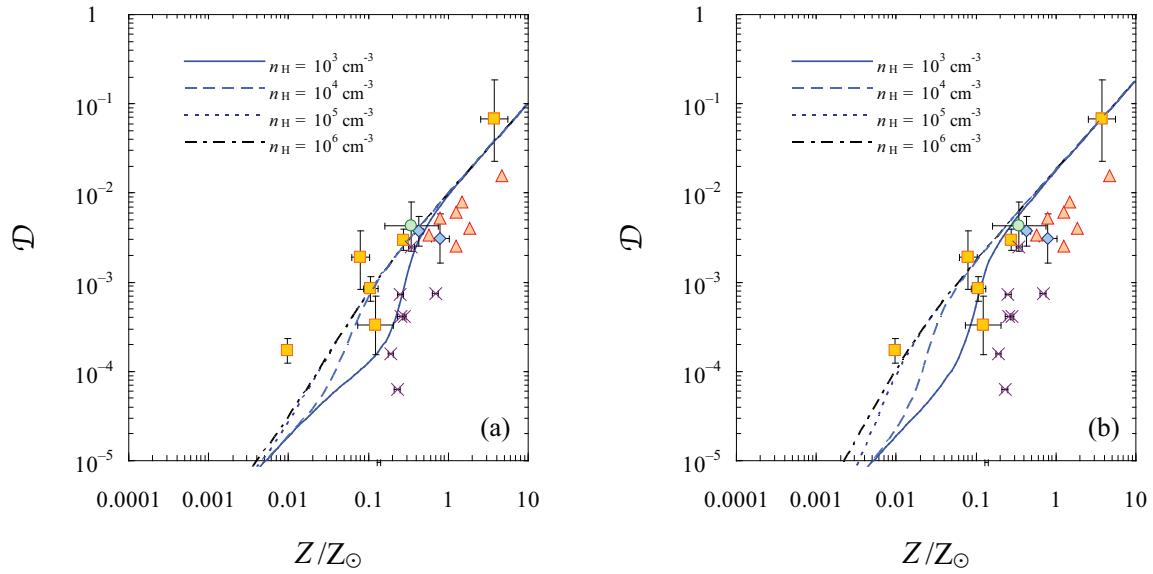

Figure 3. Same as Fig. 1, but the solid, dashed, dotted, and dot-dashed lines indicate the results with $n_{\rm H} = 10^3$, 10^4, 10^5, and 10^6 cm^{-3}, respectively, and all with $f_{\rm in} = 0.1$. Panels (a) and (b) present the results with ϵ (the star formation efficiency) $= 0.1$ and 0.01, respectively.

since we sample objects whose absorption by the ISM in the host galaxy is significantly detected. Therefore, GRBs also potentially include quiescent galaxies whose star formation efficiency is not large.

Zafar & Watson (2013) point out that in estimating the dust-to-gas ratio in nearby dwarf galaxies, we have to take into account the fact that the entire H I gas is clearly more extended than the dust emission. Indeed, Draine et al. (2007) show that, if we consider only the regions over which the dust emission is detected, a substantial fraction of interstellar dust-composing materials appears to be contained in dust. The dust mass estimate itself may also be changed: Galametz et al. (2011) show that the addition of submillimetre data results in higher dust masses than without submillimetre data. These two effects tend to make the difference in the dust-to-gas ratio between the nearby galaxy sample and the GRB sample smaller.

It is worth noting that the dust-to-metals ratios of the GRB sample is almost the same as that of the Milky Way, as pointed out by Zafar & Watson (2013). Mattsson et al. (2013) have recently shown by using an analytic model that such a 'constant dust-to-metals ratio' can be understood as the result of a balance between destruction and growth of grains in the ISM. In particular, they show that, if we consider a certain balance between grain growth and destruction, a constant dust-to-metals ratio may naturally be obtained as an asymptotic solution; i.e. the system tends to converge to a constant dust-to-metals ratio. This suggests a 'unified model' may be constructed, which can explain both the GRB sample and other data without a lot of parametric fine tuning. However, the importance of grain growth is a common feature between our model and theirs, although we did not focus on dust destruction.

6 CONCLUSION

The dust-to-gas ratios derived from GRB afterglow extinction data are excessively high such that they can be explained with an extremely efficient condensation of metals into dust in stellar ejecta, while theoretical calculations on dust formation in the wind of AGB stars and in the ejecta of SNe suggest much more moderate condensation efficiencies. We alternatively adopt a moderate condensation efficiency and a more efficient grain growth in dense clouds. Even with efficient grain growth, the excessive dust-to-gas ratio can only be explained if we assume a low star formation efficiency, which is equivalent with slow metal enrichment. Therefore, some GRB host galaxies in which most of the dust-composing metals are condensed into dust can be explained with enhanced grain growth in dense clouds, whose time-scale should be shorter than the metal enrichment time-scale (or equivalently the star formation efficiency in dense clouds is as small as $\lesssim 0.01$).

ACKNOWLEDGMENTS

We are grateful to A. K. Inoue for providing us with a compiled data set of dust formation in stellar sources. We also thank L. Mattsson, D. Watson, and A. C. Andersen for helpful discussions. This research is supported through NSC grant 99-2112-M-001-006-MY3.

REFERENCES

Asano, R., Takeuchi, T. T., Hirashita, H., & Inoue, A. K. 2013, Earth Planets Space, 65, 213
Bianchi, S., & Schneider, R. 2007, MNRAS, 378, 973
Draine, B. T., et al. 2007, ApJ, 663, 866
Dwek E., 1998, ApJ, 501, 643
Engelbracht C. W., Rieke G. H., Gordon K. D., Smith J.-D. T., Werner M. W., Moustakas J., Willmer C. N. A., Vanzi L., 2008, ApJ, 678, 804
Galametz, M., Madden, S. C., Galliano, F., Hony, S., Bendo, G. J., & Sauvage, M. 2011, A&A, 532, A56
Hirashita H., 1999, ApJ, 510, L99
Hirashita, H., & Ferrara, A. 2002, MNRAS, 337, 921
Hirashita, H., & Kuo, T.-M. 2011, MNRAS, 416, 1340

Inoue, A. K. 2003, PASJ, 55, 901
Inoue, A. K. 2011, Earth Planets Space, 63, 1027
Jones, A. P., Tielens, A. G. G. M., Hollenbach, D. J., & McKee, C. F. 1994, ApJ, 433, 797
Lisenfeld, U., & Ferrara, A. 1998, ApJ, 496, 145
Madden S., 2000, New Astron. Rev., 44, 249
Mathis, J. S., Rumpl, W., & Nordsieck, K. H. 1977, ApJ, 217, 425
Mattsson, L., et al. 2013, in preparation
Mattsson, L., & Andersen, A. C. 2012, MNRAS, 423, 38
McKee, C. F. 1989, in Allamandola L. J. & Tielens A. G. G. M. eds., IAU Symp. 135, Interstellar Dust, Kluwer, Dordrecht, 431
Nozawa, T., Kozasa, T., Habe, A., Dwek, E., Umeda, H., Tominaga, N., Maeda, K., & Nomoto, K. 2007, ApJ, 666, 955
Pei, Y. C. 1992, ApJ, 395, 130
Spitzer, L. 1978, Physical Processes in the Interstellar Medium (New York: Wiley)
Tinsley, B. M. 1980, Fundamentals of Cosmic Physics, 5, 287
Valiante, R., Schneider, R., Salvadori, S., & Bianchi, S. 2011, MNRAS, 416, 1916
Ventura, P., et al. 2012, MNRAS, 424, 2345
Vladilo, G. 2004, A&A, 421, 479
Yamasawa, D., Habe, A., Kozasa, T., Nozawa, T., Hirashita, H., Umeda, H., & Nomoto, K. 2011, ApJ, 735, 44
Yajima, H., Umemura, M., & Mori, M. 2012, MNRAS, 420, 3381
Zafar, T., & Watson, D. 2013, A&A, submitted (arXiv:1303.1141)
Zafar, T., et al. 2012, ApJ, 753, 82
Zafar, T., Watson, D., Fynbo, J. P. U., Malesani, D., Jakobsson, P., & de Ugarte Postigo, A. 2011, A&A, 532, A143
Zhukovska, S., Gail, H.-P., Trieloff, M. 2008, A&A, 479, 453

This paper has been typeset from a TEX/ LATEX file prepared by the author.